Journal of Zhejiang University-SCIENCE A (Applied Physics & Engineering)
ISSN 1673-565X (Print); ISSN 1862-1775 (Online)
www.jzus.zju.edu.cn; www.springerlink.com
E-mail: jzus@zju.edu.cn

Dynamics of a periodically driven chain of coupled nonlinear oscillators*

Paweł FRITZKOWSKI†[1], Roman STAROSTA[1], Grażyna SYPNIEWSKA-KAMIŃSKA[1], Jan AWREJCEWICZ[2]

([1]*Institute of Applied Mechanics, Poznań University of Technology, Poznań 60-965, Poland*)

([2]*Department of Automatics and Biomechanics, Technical University of Łódź, Łódź 90-924, Poland*)

E-mail: pawel.fritzkowski@put.poznan.pl

Received Sept. 15, 2016; Revision accepted Feb. 16, 2017; Crosschecked June 12, 2017

Abstract: A 1D chain of coupled oscillators is considered, including the Duffing-type nonlinearity, viscous damping, and kinematic harmonic excitation. The equations of motion are presented in a non-dimensional form. The approximate equations for the vibrational amplitudes and phases are derived by means of the classical averaging method. A simple analysis of the resulting equations allows one to determine the conditions for the two basic synchronous steady-states of the system: the in-phase and anti-phase motions. The relations between the required excitation frequency and the natural frequencies of the abbreviated (linear) system are discussed. The validity of these predictions is examined by a series of numerical experiments. The effect of the model parameters on the rate of synchronization is analyzed. For the purpose of systematic numerical studies, the cross-correlation of time-series is used as a measure of the phase adjustment between particular oscillators. Finally, some essential issues that arise in case of the mechanical system with dry friction are indicated.

Key words: Nonlinear coupled oscillators; Synchronous motion; Averaging method
http://dx.doi.org/10.1631/jzus.A1600628 **CLC number:** O313; O32

1 Introduction

In recent decades, systems of coupled oscillators have drawn the attention of many researchers. Mathematical models of such systems find applications in various areas of science and engineering, for example in physics, chemistry, and biology as well as in economy and life sciences. Usually the investigations are focused on oscillators organized in well-ordered structures: 1D chains or more complex, planar or spatial arrays. On the one hand, such multi-degree-of-freedom systems are interesting and graceful objects for purely theoretical study. On the other, results may potentially have practical implications.

Due to their complexity, i.e., a large number of components and various types of nonlinear couplings, the systems can exhibit a wide range of dynamical behaviors, e.g., regular and chaotic vibrations, bifurcations, different kinds of resonances, and synchronization (Minorsky, 1947; Nayfeh and Mook, 1995).

In particular, the problem of synchronization has been extensively analyzed over past years. Classically, the phenomenon refers to the periodic self-sustained systems (e.g., coupled oscillators of the van der Pol type). Another well-known effect is chaotic synchronization (Osipov *et al.*, 2007; Balanov *et al.*, 2009). In the former case, the averaging method is typically used to derive approximate equations that describe the oscillation amplitudes and phases. This analytical technique takes its

* Project supported by the Polish National Science Center under the Grant MAESTRO 2 (No. 2012/04/A/ST8/00738) for years 2012–2016

ORCID: Paweł FRITZKOWSKI, http://orcid.org/0000-0003-1374-2364

roots from the classical perturbation approach, and actually is the simplest variant (the first approximation) of the Krylov-Bogolyubov-Mitropolsky (KBM) method (Kryloff and Bogoliuboff, 1947; Minorsky, 1947; McLachlan, 1950; Sanders and Verhulst, 1985).

In contrast to such a meaning of synchronization, we focus on synchronous motion of a mechanical system of coupled oscillators with a periodic excitation. However, similar to the mentioned procedure for self-excited vibration, we employ the standard method of averaging, which allows us to determine the regions of in-phase and anti-phase steady-states. Next, these predictions are verified by a series of numerical experiments. Moreover, since such oscillatory chains are relatively rarely considered including motion-dependent discontinuities, some brief remarks on the synchronous vibration of the system with dry friction are presented.

Classical theoretical studies are concerned mainly with synchronization due to appropriate external periodic forcing. This concept has a rather limited range of applicability. Nowadays, researchers focus on automatic control of synchronization phenomena, and this is a more flexible and efficient approach. There are various control methods that usually are designed or adapted for specific types of systems, e.g., coupled Poincaré, Rössler or Lorenz oscillators (Belykh *et al.*, 2005; Osipov *et al.*, 2007). In what follows, our investigations are restricted to the classical approach.

2 Mathematical model

Consider a 1D chain of coupled oscillators illustrated in Fig. 1. The system consists of n rigid bodies of mass m_i interconnected by nonlinear springs with stiffness constants k_i and k_i', and viscous dampers characterized by coefficients c_i. The particles can slide on the ground; basically, the contact will be treated as frictionless. The farthest left body in the scheme is an additional oscillator that undergoes an imposed harmonic motion. It is attached to the system, and thus it is a source of kinematic excitation.

Let x_i denote the displacement of the ith component from its equilibrium position. The exciter is assumed to move with an amplitude A_0 and an angular frequency ω_{ex}:

$$x_0(t) = A_0 \cos(\omega_{\mathrm{ex}} t). \tag{1}$$

The kinetic and potential energies of the system are respectively given by

$$T = \frac{1}{2}\sum_{i=1}^{n} m_i \dot{x}_i^2, \tag{2}$$

$$V = \frac{1}{2}\sum_{i=1}^{n} k_i (x_i - x_{i-1})^2 + \frac{1}{4}\sum_{i=1}^{n} k_i' (x_i - x_{i-1})^4. \tag{3}$$

Moreover, the Rayleigh dissipation function can be expressed as

$$R = \frac{1}{2}\sum_{i=1}^{n} c_i (\dot{x}_i - \dot{x}_{i-1})^2. \tag{4}$$

By introducing the Lagrangian $L = T - V$, the Lagrange equations for a dissipative material system take the form of

$$\frac{\mathrm{d}}{\mathrm{d}t}\left(\frac{\partial L}{\partial \dot{q}_i}\right) - \frac{\partial L}{\partial q_i} + \frac{\partial R}{\partial \dot{q}_i} = 0, \quad i = 1, 2, \cdots, n, \tag{5}$$

where q_i denotes the ith generalized coordinate, and n is the number of degrees of freedom of the system. Taking $q_i = x_i$, one can obtain the following equations of motion for the considered chain:

$$\begin{aligned} m_i\ddot{x}_i &+ k_i(x_i - x_{i-1}) - k_{i+1}(x_{i+1} - x_i) \\ &+ k_i'(x_i - x_{i-1})^3 - k_{i+1}'(x_{i+1} - x_i)^3 \\ &+ c_i(\dot{x}_i - \dot{x}_{i-1}) - c_{i+1}(\dot{x}_{i+1} - \dot{x}_i) = 0, \\ m_n\ddot{x}_n &+ k_n(x_n - x_{n-1}) + k_n'(x_n - x_{n-1})^3 \\ &+ c_n(\dot{x}_n - \dot{x}_{n-1}) = 0, \end{aligned} \tag{6}$$

where $i = 1, 2, \cdots, n-1$.

Let us define the reference frequency, dimensionless time, and the static deflection of the first spring, respectively (under the first mass only):

$$\omega_{\mathrm{r}}^2 = \frac{k_1}{m_1}, \quad \tau = \omega_{\mathrm{r}} t, \quad x_{1\mathrm{st}} = \frac{m_1 g}{k_1}.$$

Now, the mathematical model can be transformed to the non-dimensional form ($i = 1, 2, \cdots, n$):

$$\begin{aligned} \ddot{X}_i &+ \omega_i^2 X_i = \alpha_{i,i-1} X_{i-1} + \alpha_{i,i+1} X_{i+1} \\ &- \beta_{i,i-1}(X_i - X_{i-1})^3 + \beta_{i,i+1}(X_{i+1} - X_i)^3 \\ &- \gamma_{i,i-1}(\dot{X}_i - \dot{X}_{i-1}) + \gamma_{i,i+1}(\dot{X}_{i+1} - \dot{X}_i), \end{aligned} \tag{7}$$

where $X_i = x_i / x_{1\mathrm{st}}$ and

$$X_0 = a_0 \cos(\Omega_{\mathrm{ex}} \tau), \quad a_0 = \frac{A_0}{x_{1\mathrm{st}}}, \quad \Omega_{\mathrm{ex}} = \frac{\omega_{\mathrm{ex}}}{\omega_{\mathrm{r}}},$$

$$\omega_i^2 = \alpha_{i,i-1} + \alpha_{i,i+1},$$

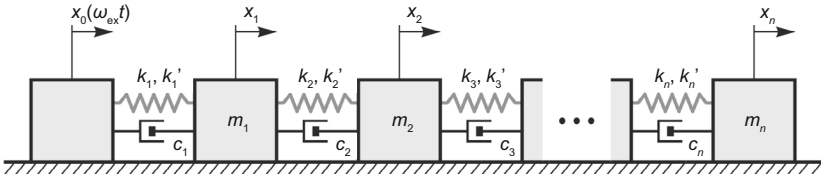

Fig. 1 The 1D chain-like mechanical system

$$\alpha_{i,i-1}=\frac{k_i}{m_i\omega_{\mathrm{r}}^2},\quad \alpha_{i,i+1}=\frac{k_{i+1}}{m_i\omega_{\mathrm{r}}^2},$$
$$\beta_{i,i-1}=\frac{k_i' x_{1\mathrm{st}}^2}{m_i\omega_{\mathrm{r}}^2},\quad \beta_{i,i+1}=\frac{k_{i+1}' x_{1\mathrm{st}}^2}{m_i\omega_{\mathrm{r}}^2},$$
$$\gamma_{i,i-1}=\frac{c_i}{m_i\omega_{\mathrm{r}}},\quad \gamma_{i,i+1}=\frac{c_{i+1}}{m_i\omega_{\mathrm{r}}}.$$

Specifically,

$$\alpha_{n,n+1}=\beta_{n,n+1}=\gamma_{n,n+1}=0,$$

so that the related terms in Eq. (7) vanish for the last oscillator ($i=n$). An overdot in Eq. (7) denotes differentiation with respect to τ. The sets of coefficients $\alpha_{i,i-1}$, $\beta_{i,i-1}$, $\gamma_{i,i-1}$ and $\alpha_{i,i+1}$, $\beta_{i,i+1}$, $\gamma_{i,i+1}$ correspond to the interactions of the ith particle with the left and right neighbors, respectively. The basic frequency ω_i is the natural frequency for a single uncoupled oscillator.

We restrict our attention to dynamics of the system with the following initial conditions:

$$X_i(0)=X_{i0},\quad \dot{X}_i(0)=0,\quad i=1,\,2,\,\cdots,\,n, \tag{8}$$

where X_{i0} is the imposed initial displacement.

3 Analytical studies

3.1 Averaging procedure

For convenience of analysis, let us introduce formally the small parameter $0<\varepsilon\ll 1$ to the equations of motion:

$$\ddot{X}_i+\omega_i^2 X_i=\alpha_i(\tau,\,X_j)+\varepsilon f_i(\tau,\,X_j,\,\dot{X}_j), \tag{9}$$

where $i=1,\,2,\,\cdots,\,n$ and $j=i-1,\,i,\,i+1$. The right-hand side functions α_i relate to the linear part of the stiffness coupling. Functions f_i, in turn, include the viscous and cubic terms. In the case of weak nonlinearity and weak damping, the parameters β_{ij} and γ_{ij} are small themselves. However, they can be expressed by

$$\beta_{ij}=\varepsilon\tilde{\beta}_{ij},\quad \gamma_{ij}=\varepsilon\tilde{\gamma}_{ij}, \tag{10}$$

and f_i can be considered to involve the new parameters $\tilde{\beta}_{ij}$, $\tilde{\gamma}_{ij}$.

We apply the classical method of averaging (Kryloff and Bogoliuboff, 1947; Minorsky, 1947; McLachlan, 1950); thus, the trial solutions are assumed in the form of

$$X_i(\tau)=a_i(\tau)\cos\psi_i(\tau), \tag{11}$$
$$\psi_i(\tau)=\Omega_{\mathrm{ex}}\tau+\phi_i(\tau), \tag{12}$$

where ϕ_i represents the phase angle. The amplitudes a_i and total phases ψ_i are regarded as slowly varying with time. As in the linear case ($\varepsilon=0$), the velocities are taken as

$$\dot{X}_i=-a_i\Omega_{\mathrm{ex}}\sin(\Omega_{\mathrm{ex}}\tau+\phi_i), \tag{13}$$

and hence the following conditions must be satisfied:

$$\dot{a}_i\cos(\Omega_{\mathrm{ex}}\tau+\phi_i)-a_i\dot{\phi}\sin(\Omega_{\mathrm{ex}}\tau+\phi_i)=0. \tag{14}$$

Differentiating Eq. (13) gives

$$\begin{aligned}\ddot{X}_i=&-\dot{a}_i\Omega_{\mathrm{ex}}\sin(\Omega_{\mathrm{ex}}\tau+\phi_i)\\&-a_i\Omega_{\mathrm{ex}}(\Omega_{\mathrm{ex}}+\dot{\phi})\cos(\Omega_{\mathrm{ex}}\tau+\phi_i).\end{aligned} \tag{15}$$

Substituting Eqs. (11), (13), and (15) into the system Eq. (9) for $i=1,\,2,\,\cdots,\,n$, we obtain a set of n equations. Together with conditions Eq. (14), they form a system that can be solved for $\dot{a}_i$ and $\dot{\phi}_i$:

$$\begin{cases}\dot{a}_i=g_i(\tau,\,a_j,\,\phi_j),\\ \dot{\phi}_i=h_i(\tau,\,a_j,\,\phi_j),\end{cases}\quad j=i-1,\,i,\,i+1. \tag{16}$$

Treating a_j and ϕ_j as constants over the period $T=2\pi/\Omega_{\mathrm{ex}}$, the averaging procedure can be performed for Eq. (16):

$$\begin{cases}\dot{a}_i=\overline{g}_i(a_j,\,\phi_j)=\frac{1}{T}\int\limits_{\tau}^{\tau+T} g_i(\tau,\,a_j,\,\phi_j)\,\mathrm{d}\tau,\\ \dot{\phi}_i=\overline{h}_i(a_j,\,\phi_j)=\frac{1}{T}\int\limits_{\tau}^{\tau+T} h_i(\tau,\,a_j,\,\phi_j)\,\mathrm{d}\tau.\end{cases} \tag{17}$$

For the chain system, the averaged equations describing the slow variations of amplitudes and phases become

$$\begin{aligned}\dot{a}_i = &-\frac{\alpha_{i,i-1}}{2\Omega_{\mathrm{ex}}}a_{i-1}S_i + \frac{\alpha_{i,i+1}}{2\Omega_{\mathrm{ex}}}a_{i+1}S_{i+1}\\ &-\frac{3\beta_{i,i-1}}{8\Omega_{\mathrm{ex}}}a_{i-1}S_i\left(a_{i-1}^2+a_i^2-2a_{i-1}a_iC_i\right)\\ &+\frac{3\beta_{i,i+1}}{8\Omega_{\mathrm{ex}}}a_{i+1}S_{i+1}\left(a_{i+1}^2+a_i^2-2a_{i+1}a_iC_{i+1}\right)\\ &-\frac{\gamma_{i,i-1}}{2}\left(a_i-a_{i-1}C_i\right)-\frac{\gamma_{i,i+1}}{2}\left(a_i-a_{i+1}C_{i+1}\right),\end{aligned} \tag{18}$$

$$\begin{aligned}\dot{\phi}_i = &\,\Delta_i-\frac{\alpha_{i,i-1}}{2\Omega_{\mathrm{ex}}a_i}C_i-\frac{\alpha_{i,i+1}}{2\Omega_{\mathrm{ex}}a_i}C_{i+1}\\ &+\frac{3\beta_{i,i-1}}{8\Omega_{\mathrm{ex}}a_i}\left(2a_{i-1}^2a_i+a_i^3-a_{i-1}^3C_i-3a_{i-1}a_i^2C_i\right.\\ &\left.+a_{i-1}^2a_iC_{2,i}\right)+\frac{3\beta_{i,i+1}}{8\Omega_{\mathrm{ex}}a_i}\left(2a_{i+1}^2a_i+a_i^3\right.\\ &\left.-a_{i+1}^3C_{i+1}-3a_{i+1}a_i^2C_{i+1}+a_{i+1}^2a_iC_{2,i+1}\right)\\ &-\frac{\gamma_{i,i-1}a_{i-1}}{2a_i}S_i+\frac{\gamma_{i,i+1}a_{i+1}}{2a_i}S_{i+1},\end{aligned} \tag{19}$$

where $\theta_i=\phi_i-\phi_{i-1}$ denotes the phase differences ($\phi_0=0$) and the auxiliary symbols are used:

$$S_j=\sin\theta_j,\quad C_j=\cos\theta_j,\quad C_{2,j}=\cos(2\theta_j),$$

for $j=i,\,i+1$. Δ_i denotes the frequency detuning parameter:

$$\Delta_i=\frac{\omega_i^2-\Omega_{\mathrm{ex}}^2}{2\Omega_{\mathrm{ex}}}. \tag{20}$$

Note that if the basic and forcing frequencies are close ($\omega_i\approx\Omega_{\mathrm{ex}}$), then $\Delta_i\approx\omega_i-\Omega_{\mathrm{ex}}$. As can be seen, the nonlinear autonomous system Eqs. (18) and (19) have a quite complex form. However, it allows for the analysis of conditions for synchronous states.

Numerical solutions of the equations of motion and the averaged system for $n=3$ coupled oscillators are compared in Fig. 2. Results are obtained for the following exemplary values of the dimensional parameters:

$$\begin{gathered}m_1=m_3=1\,\mathrm{kg},\quad m_2=4m_1,\\ k_1=20\,\mathrm{N/m},\quad k_2=2k_1,\quad k_3=4k_1\\ k_1'=k_3'=10\,\mathrm{N/m^3},\quad k_2'=2k_1',\\ c_i=0.2\,\mathrm{N{\cdot}s/m},\quad \omega_{\mathrm{ex}}=2\pi\,\mathrm{rad/s},\end{gathered}$$

and the initial relative amplitudes:

$$a_0=1,\quad a_{i0}=X_{i0}=0.5.$$

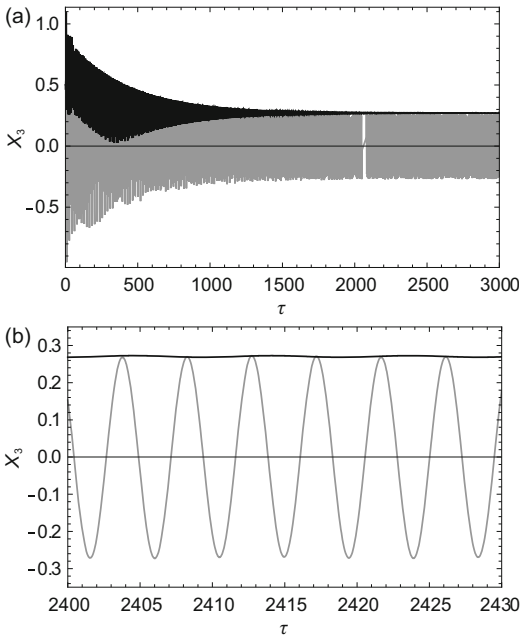

Fig. 2 Response of the third oscillator: overall view (a) and detailed view (b) of numerical solution (grey) and the amplitude evaluated using the averaged system (black)

For such data the nonlinear and dissipative couplings are not strong, for instance $\alpha_{12}=2$, $\beta_{12}\approx0.241$, $\gamma_{12}\approx0.045$ or $\alpha_{21}=0.5$, $\beta_{21}\approx0.06$, $\gamma_{21}\approx0.011$. Fig. 3 presents time history of the responses X_1, X_2, and X_3. Errors of the averaging-based solutions are shown in Fig. 4, i.e., the difference between the purely numerical solution of the equations of motion ($\widetilde{X}_i$) and X_i approximated by Eq. (11):

$$e_i=\widetilde{X}_i-X_i. \tag{21}$$

Taking into account the vibration amplitudes of particular oscillators (Fig. 3), the errors do not exceed 3%.

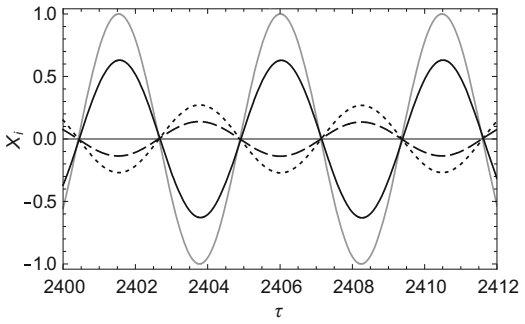

Fig. 3 Time history of excitation X_0 (grey) and responses of particular oscillators (black): X_1 (solid), X_2 (dashed), and X_3 (dotted)

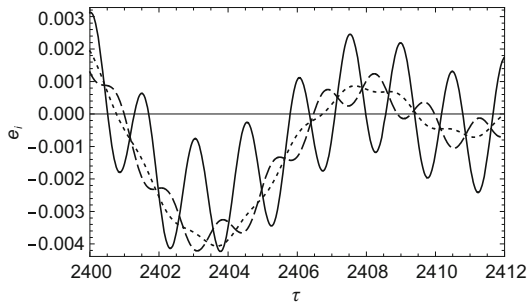

Fig. 4 Errors of the averaging-based solutions: e_1 (solid), e_2 (dashed), and e_3 (dotted)

3.2 Synchronous motion of the system

We focus on phase synchronization of all oscillators and the exciter. Thus, the steady-state solutions fulfilling

$$\dot{a}_i = 0, \quad \dot{\theta}_i = 0, \quad i = 1, 2, \cdots, n \tag{22}$$

are sought. Satisfying the second set of equations ensures a uniform phase shift between oscillators. However, the condition can be replaced with

$$\dot{\phi}_i = 0, \quad i = 1, 2, \cdots, n, \tag{23}$$

if the frequency locking effect is expected ($\dot{\psi}_i = \Omega_{\mathrm{ex}}$). Particularly, two basic synchronous states are taken into account: in-phase and anti-phase oscillations, which implies $\theta_i = 0$ and $\theta_i = \pi$ ($i = 1, 2, \cdots, n$), respectively.

For simplicity, let us consider the system with $n = 3$ members only. First, the subsystem Eq. (18) is analyzed by putting $\dot{a}_i = 0$:

1. For $\theta_i = 0$ we have

$$\begin{cases} \gamma_{1,0}(a_0 - a_1) + \gamma_{1,2}(a_2 - a_1) = 0, \\ \gamma_{2,1}(a_1 - a_2) + \gamma_{2,3}(a_3 - a_2) = 0, \\ \gamma_{3,2}(a_2 - a_3) = 0. \end{cases} \tag{24}$$

As can be seen, all the terms are of order ε. The equations are satisfied exactly for $a_i = a_{i-1}$ ($i = 1, 2, \cdots, n$), that finally leads to $a_i = a_0$. Thus, theoretically completely synchronous motion can be observed (identical phases and amplitudes).

2. For $\theta_i = \pi$ we arrive at

$$\begin{cases} \gamma_{1,0}(a_0 + a_1) + \gamma_{1,2}(a_2 + a_1) = 0, \\ \gamma_{2,1}(a_1 + a_2) + \gamma_{2,3}(a_3 + a_2) = 0, \\ \gamma_{3,2}(a_2 + a_3) = 0. \end{cases} \tag{25}$$

Solving the system gives $a_i = -a_{i-1}$ for $i = 1, 2, \cdots, n$. If each a_i is considered to be a real coefficient (the amplitude value with a sign), the result confirms the anti-phase oscillations and indicates equal magnitudes of all the amplitudes.

More information can be found from an analysis of the subsystem Eq. (19) when taking $\dot{\phi}_i = 0$:

1. For $\theta_i = 0$ and $a_i = a_0$ we have

$$\begin{cases} \alpha_{1,0} + \alpha_{1,2} - \omega_1^2 + \Omega_{\mathrm{ex}}^2 = 0, \\ \alpha_{2,1} + \alpha_{2,3} - \omega_2^2 + \Omega_{\mathrm{ex}}^2 = 0, \\ \alpha_{3,2} - \omega_3^2 + \Omega_{\mathrm{ex}}^2 = 0. \end{cases} \tag{26}$$

When taking into account the parameters definitions, the system reduces to the condition $\Omega_{\mathrm{ex}}^2 = 0$. As $\Omega_{\mathrm{ex}} \to 0$, the chain of oscillators tends to the synchronous state, which is the result that one might intuitively expect for very slow excitation.

2. For $\theta_i = \pi$ and $a_i = a_0$ we arrive at

$$\begin{cases} \alpha_{1,0} + \alpha_{1,2} + 6a_0^2(\beta_{1,0} + \beta_{1,2}) + \omega_1^2 - \Omega_{\mathrm{ex}}^2 = 0, \\ \alpha_{2,1} + \alpha_{2,3} + 6a_0^2(\beta_{2,1} + \beta_{2,3}) + \omega_2^2 - \Omega_{\mathrm{ex}}^2 = 0, \\ \alpha_{3,2} + 6a_0^2\beta_{3,2} + \omega_3^2 - \Omega_{\mathrm{ex}}^2 = 0, \end{cases} \tag{27}$$

or

$$\begin{cases} 2(\alpha_{1,0} + \alpha_{1,2}) + 6a_0^2(\beta_{1,0} + \beta_{1,2}) - \Omega_{\mathrm{ex}}^2 = 0, \\ 2(\alpha_{2,1} + \alpha_{2,3}) + 6a_0^2(\beta_{2,1} + \beta_{2,3}) - \Omega_{\mathrm{ex}}^2 = 0, \\ 2\alpha_{3,2} + 6a_0^2\beta_{3,2} - \Omega_{\mathrm{ex}}^2 = 0. \end{cases} \tag{28}$$

If the frequency Ω_{ex} plays the role of a control parameter, one can obtain

$$\begin{cases} \Omega_{\mathrm{ex}} = \sqrt{2}\sqrt{\alpha_{1,0} + \alpha_{1,2} + 3a_0^2(\beta_{1,0} + \beta_{1,2})}, \\ \Omega_{\mathrm{ex}} = \sqrt{2}\sqrt{\alpha_{2,1} + \alpha_{2,3} + 3a_0^2(\beta_{2,1} + \beta_{2,3})}, \\ \Omega_{\mathrm{ex}} = \sqrt{2}\sqrt{\alpha_{3,2} + 3a_0^2\beta_{3,2}}. \end{cases} \tag{29}$$

The basic way to satisfy all these conditions is to ensure the sameness of all oscillators:

$$\begin{cases} \alpha_{1,0} + \alpha_{1,2} = \alpha_{2,1} + \alpha_{2,3} = \alpha_{3,2}, \\ \beta_{1,0} + \beta_{1,2} = \beta_{2,1} + \beta_{2,3} = \beta_{3,2}. \end{cases} \tag{30}$$

In the next section, the ability to generate the two synchronous states of the system will be verified in a number of numerical experiments.

4 Numerical studies

4.1 Mechanical system without friction

For simplicity, the quality of the predictions which is obtained by means of the averaging method is examined for chains of identical oscillators. Let α, β, and γ denote coefficients related to the uniform properties: linear stiffness, nonlinear stiffness, and viscous damping, i.e.,

$$\begin{cases} \alpha = \alpha_{1,0} = \alpha_{1,2} = \alpha_{2,1} = \alpha_{2,3} = \cdots = 2\alpha_{n,n-1}, \\ \beta = \beta_{1,0} = \beta_{1,2} = \beta_{2,1} = \beta_{2,3} = \cdots = 2\beta_{n,n-1}, \\ \gamma = \gamma_{1,0} = \gamma_{1,2} = \gamma_{2,1} = \gamma_{2,3} = \cdots = 2\gamma_{n,n-1}, \end{cases} \tag{31}$$

which leads to identical frequency detuning:

$$\Delta = \Delta_1 = \Delta_2 = \cdots = \Delta_n. \tag{32}$$

The following values of the dimensionless parameters are treated as the basic data set:

$$\alpha = 1, \quad \beta = 0.1, \quad \gamma = 0.02, \tag{33}$$

$$a_0 = 0.5, \quad X_{i0} = 0.25. \tag{34}$$

According to the analytical results, the excitation frequency should be set close to the values

$$\Omega_{\mathrm{ex}}^{(1)} = 0 \ \text{ and } \ \Omega_{\mathrm{ex}}^{(2)} = 2\sqrt{\alpha + 3a_0^2\beta}, \tag{35}$$

which are related to the two vibration regimes: in-phase and anti-phase motions, respectively.

To assess relevance of these specific frequency selections, we consider a linear system ($\beta = 0$) of $n = 3$ oscillators. In such case, the amplitudes of the system steady-state response can be easily determined analytically. For the in-phase motion ($\theta_i = 0$), for example, one can see that

$$\begin{cases} a_1 = \frac{2(\Delta+\gamma)^2\Omega_{\mathrm{ex}}^2 + (\alpha+\gamma\Omega_{\mathrm{ex}})^2}{(\Delta+\gamma)\Omega_{\mathrm{ex}}} A, \\ a_2 = (\alpha + \gamma\Omega_{\mathrm{ex}})A, \\ a_3 = \frac{(\alpha+\gamma\Omega_{\mathrm{ex}})^2}{(\Delta+\gamma)\Omega_{\mathrm{ex}}} A, \end{cases} \tag{36}$$

where

$$A = \frac{a_0(\alpha + \gamma\Omega_{\mathrm{ex}})}{(4\Delta^2 + 8\gamma\Delta + \gamma^2)\Omega_{\mathrm{ex}}^2 - 3\alpha^2 - 6\alpha\gamma\Omega_{\mathrm{ex}}}. \tag{37}$$

Fig. 5a illustrates the dependence of the oscillators amplitudes a_1, a_2, and a_3 on the model parameters. The vertical asymptotes correspond to the natural frequencies of the system:

$$\Omega_1 \approx 0.52, \quad \Omega_2 \approx 1.41, \quad \Omega_3 \approx 1.93. \tag{38}$$

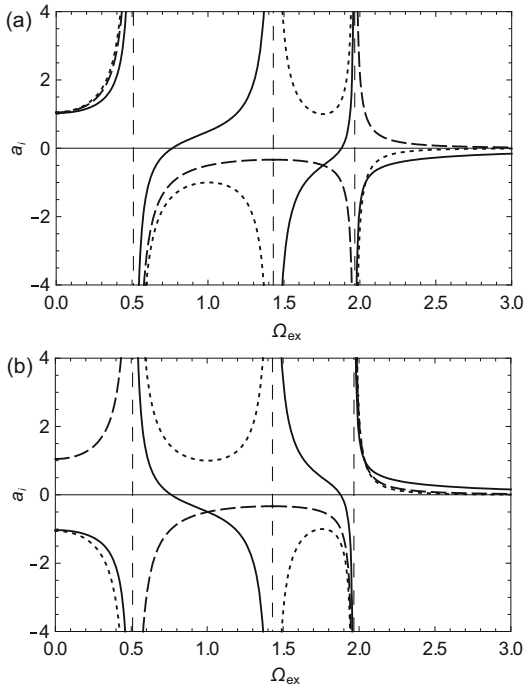

Fig. 5 Amplitudes of particular oscillators in the linear case with the assumption of in-phase (a) and anti-phase (b) vibrations: a_1 (solid), a_2 (dashed), and a_3 (dotted)

As can be seen, only the excitation with $\Omega_{\mathrm{ex}} < \Omega_1$ may produce the in-phase vibrations with approximately identical amplitudes. Similar 'amplitude–excitation frequency' curves for the second synchronous state are plotted in Fig. 5b. Note that the anti-phase character of motion is taken into account by putting $\theta_i = \pi$. Therefore, the possibility of anti-phase motion is indicated by all coefficients a_i with the same sign, achievable in the region for $\Omega_{\mathrm{ex}} > \Omega_3$.

Generally, for arbitrary n, the in-phase solutions may be observed as $\Omega_{\mathrm{ex}} < \Omega_1$, i.e., below the first natural frequency related to the in-phase vibrational normal mode. The system may be forced to come into anti-phase, in turn, if $\Omega_{\mathrm{ex}} > \Omega_n$, i.e., above the last natural frequency that always corresponds to the out-of-phase normal mode. These considerations are appropriate for the linear case. However, the conclusions based on the abbreviated (linear) system are presumably applicable also to the full, weakly nonlinear (quasi-linear) one.

The responses of the system for $n = 3$ within the two discussed regimes are shown in Fig. 6. For $\Omega_{\mathrm{ex}} = 0.4$, vibrations of all oscillators are phase-synchronized with the excitation, while the

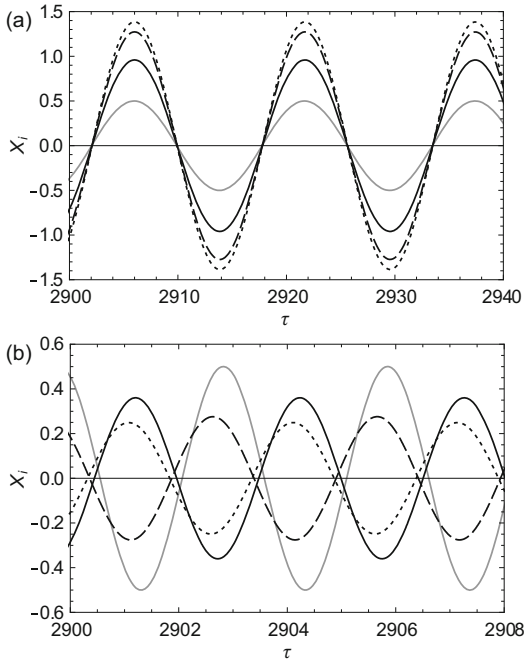

Fig. 6 Vibrations of the system ($n = 3$) for $\Omega_{ex} = 0.4$ (a) and $\Omega_{ex} = 2.074$ (b): X_0 (solid, grey), X_1 (solid, black), X_2 (dashed), and X_3 (dotted)

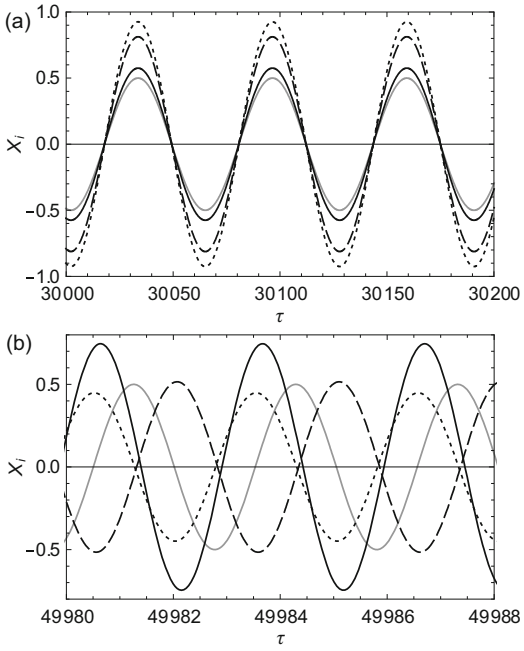

Fig. 7 Vibrations of the system ($n = 10$): (a) $\Omega_{ex} = 0.1$; X_0 (solid, grey), X_1 (solid, black), X_5 (dashed), and X_{10} (dotted); (b) $\Omega_{ex} = 2.074$; X_0 (solid, grey), $X_8 \times 10^2$ (solid, black), $X_9 \times 10^2$ (dashed), and $X_{10} \times 10^2$ (dotted)

amplitude magnitudes differ from each other and are much greater than a_0. However, a series of numerical simulations demonstrate that a decrease (Ω_{ex} towards 0) gradually adjusts the amplitudes, too ($a_i \to a_0$).

In the less trivial case ($\Omega_{ex} = 2.074$), the system behavior can be classified as anti-phase motion, although there is a small but noticeable phase shift between every element and the excitation (Fig. 6b). More precisely, some phase differences occur between each pair of neighbors, and the shift cumulates along the chain. Thus, the third and second oscillators, for instance, are better synchronized than the third one and the excitation. It seems to be quite obvious that the effect may become stronger as n increases.

Analogous results for a longer chain ($n = 10$) are presented in Fig. 7. It should be noted that in this case, $\Omega_1 \approx 0.16$ and $\Omega_{10} \approx 1.99$, and thus the first natural frequency of the linear system is much lower than that for $n = 3$. Since differences between the amplitudes of adjacent oscillators are relatively small, the in-phase state X_i is visualized for $i = 1, 5, 10$. Again, all amplitudes tend to a_0 for decreasing Ω_{ex}.

When it comes to the anti-phase vibrations, the time history of X_i for $i = 8, 9, 10$ is shown. The system exhibits a cumulative phase shift between particular oscillators and the excitation, which becomes the largest just for the last member. However, the rate of mutual synchronization (between the neighbors) remains very strong. Last but not least, one can observe a significant decline in amplitudes. Note that displacements X_8, X_9, and X_{10} are two orders of magnitude smaller than X_0.

It can be supposed that changes in values of the model parameters affect the adjustment between X_0 and $X_1, X_2, \cdots, X_n$. For the purpose of more systematic numerical studies, the cross-correlation between time series is applied:

$$r_{i,j}(\Delta\tau_J) = \sum_I X_i(\tau_I) X_j(\tau_I - \Delta\tau_J), \tag{39}$$

where the uppercase indices I, J refer to time points. If h denotes the step size, then

$$\tau_I = Ih, \quad \Delta\tau_J = Jh, \quad I \geq J. \tag{40}$$

The cross-correlation is computed over at least one period of steady-state response X_i, after omitting the range of transient motion. Hence, the summation in Eq. (39) is conducted for large I while $J \ll I$ ($0 \leq \tau_J \leq T$). The defined quantity $r_{i,j}$ can be treated

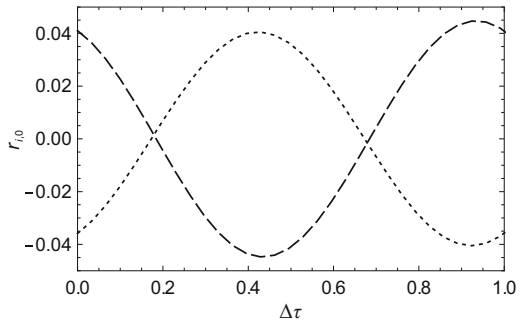

Fig. 8 Cross-correlation between X_0 and X_2 (dashed), and between X_0 and X_3 (dotted) ($n = 3$ and $\Omega_{ex} = 2.074$)

as a measure of the synchronization rate between X_i and X_j.

As an example, Fig. 8 illustrates the cross-correlation functions for the pairs $i = 2$, $j = 0$ and $i = 3$, $j = 0$ in the case shown in Fig. 6b. It must be emphasized that the horizontal axis of the plot represents the relative time shift, i.e., $\Delta\tau = \Delta\tau_J/T$. When both the oscillator and the exciter move in phase, $r_{i,j}$ reaches its maximum near $\Delta\tau = 0$ or $\Delta\tau = 1$. For X_2 and X_0, the maximal value $r_{\max} \approx 0.045$ corresponds to $\Delta\tau_{\max} \approx 0.92$, which indicates that solution X_2 is slightly shifted left (by $0.08T$) with respect to X_0. In the anti-phase case, in turn, the maximum of $r_{i,j}$ should occur near $\Delta\tau = 0.5$. For X_3 and X_0, we obtain $r_{\max} \approx 0.041$ and $\Delta\tau_{\max} \approx 0.43$, which confirms that the ideal anti-phase motion would be observed, if X_0 is shifted to the left by $0.07\,T$ (Fig. 6b).

The effect of a_0, α, β, and γ on time shift $\Delta\tau_{\max}$ related to $n = 3$ members of the system is graphically presented in Fig. 9. The analysis of $r_{i,0}$ is performed for the following ranges and steps of the parameters:

$$\begin{cases} 0.05 \le a_0 \le 2, & \Delta a_0 = 0.01, \\ 0.1 \le \alpha \le 3, & \Delta\alpha = 0.02, \\ 0 \le \beta \le 0.5, & \Delta\beta = 0.005, \\ 0.002 \le \gamma \le 0.2, & \Delta\gamma = 0.002. \end{cases}$$

Numerical solutions are computed sequentially four times, i.e., one parameter is varied when the others are held fixed at the values given in Eq. (33). Only the less trivial, anti-phase case is investigated. For every value of the amplitude a_0 and the stiffness coefficients α and β, the excitation frequency is calculated based on Eq. (35). Generally, the phase adjustment remains at a high level, but it can be slightly improved by increasing a_0 or β. At the same time, larger values of the damping coefficient γ have a negative influence on the quality of synchronous motion. The latter effect is especially evident for $i > 1$. Finally, the system is almost insensitive to changes of the stiffness α. However, a sharp fall in $\Delta\tau_{\max}$ at $\alpha \approx 1.4$ suggests that the weak linear coupling is an indispensable factor for synchronization.

Similar characteristics are obtained for $n = 10$. They are depicted in Fig. 10 for the three last oscillators ($i = 8$, 9, 10). The time shift reaches smaller values when compared with the previous case. However, the most sudden increase in the phase adjustment can be observed in the ranges of relatively low values of a_0 and β ($a_0 < 0.5$, $\beta < 0.1$). Needless to say, the negative effect of γ intensifies with increasing n. In case of α, in turn, no rapid changes occur in $\Delta\tau_{\max}$.

It is worth mentioning that such numerical studies are also conducted for the mutual synchronization of oscillators, i.e., cross-correlation $r_{i,i-1}$ is analyzed. The phase adjustment between the neighbors remains strong: $0.44 < \Delta\tau_{\max} < 0.56$ in the whole ranges of a_0 and β. The time shift tends to lower values for higher damping ($\gamma > 0.1$). Nevertheless, the decrease is considerably weaker than that in case of $r_{i,0}$.

The results may seem to provide an interesting and simple recipe for improvement of the adjustment rate between the oscillators and excitation. Unfortunately, there is another effect of a significant increase of parameters a_0 and β: a drastic decline in the vibration amplitudes. As can be seen from Figs. 11a and 11c (p.506), the maximum cross-correlation between X_{10} and X_0 drops to very low values for $a_0 > 1$ and $\beta > 0.2$. Such behavior of $r_{\max}$ indicates extremely small displacements of the last member. Naturally, decreasing viscous damping, advantageous for the phase adjustment, leads to a stronger response X_{10} (Fig. 11d). The stiffness α is the only parameter whose growth constantly intensifies the vibrations.

For instance, the consequences of an increase in the excitation amplitude from $a_0 = 0.5$ to $a_0 = 0.8$ can be seen in Fig. 12 (p.506). In comparison with the case shown in Fig. 7b, the solutions X_8, X_9, and X_{10} are better adjusted to X_0. However, now they are an order of magnitude smaller than before, and in the graph they need to be scaled by a factor of 10^3.

It should be noted that a series of numerical

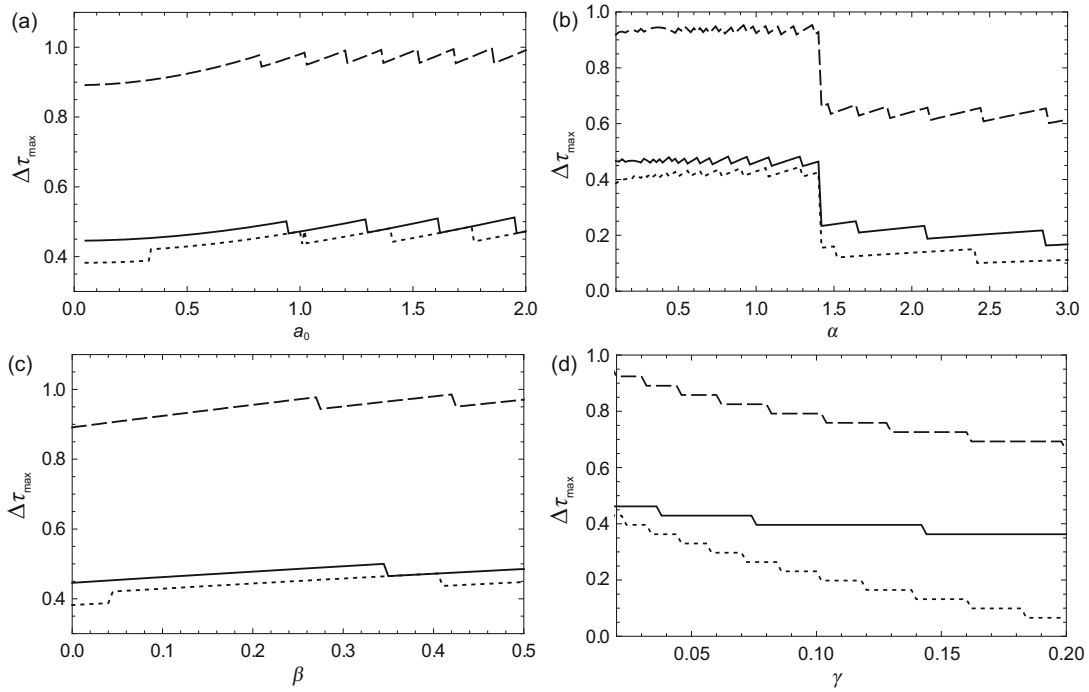

Fig. 9 Effect of parameters a_0 (a), α (b), β (c), and γ (d) on synchronous motion of the oscillators and the excitation ($n = 3$): time shift for X_1 (solid), X_2 (dashed), and X_3 (dotted)

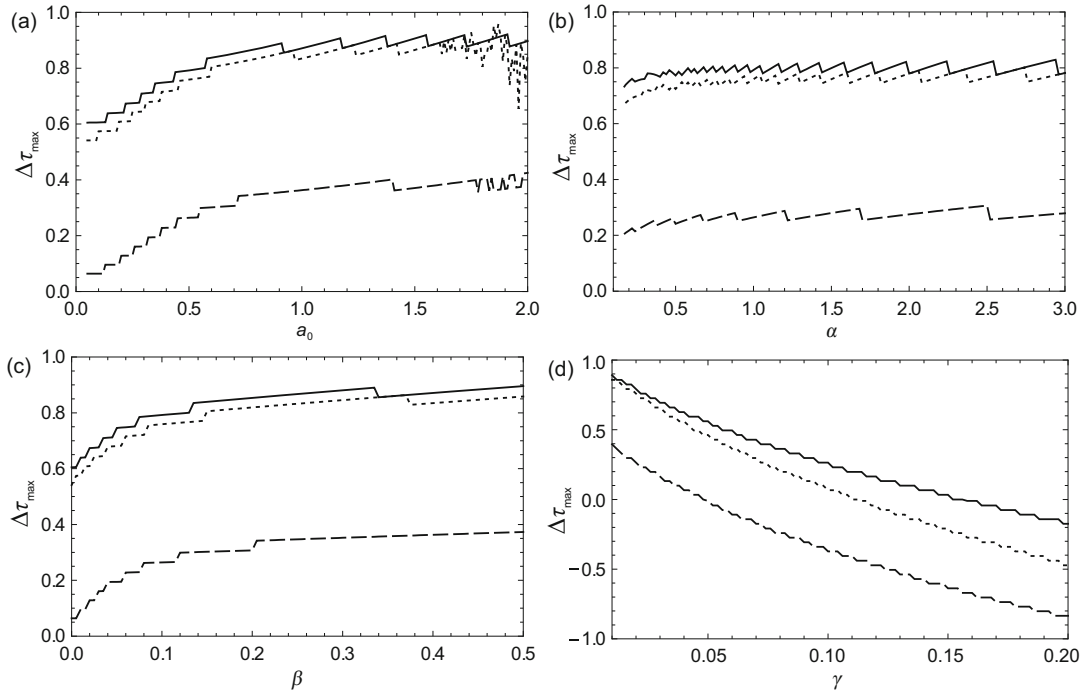

Fig. 10 Effect of parameters a_0 (a), α (b), β (c), and γ (d) on synchronous motion of the oscillators and the excitation ($n = 10$): time shift for X_8 (solid), X_9 (dashed), and X_{10} (dotted)

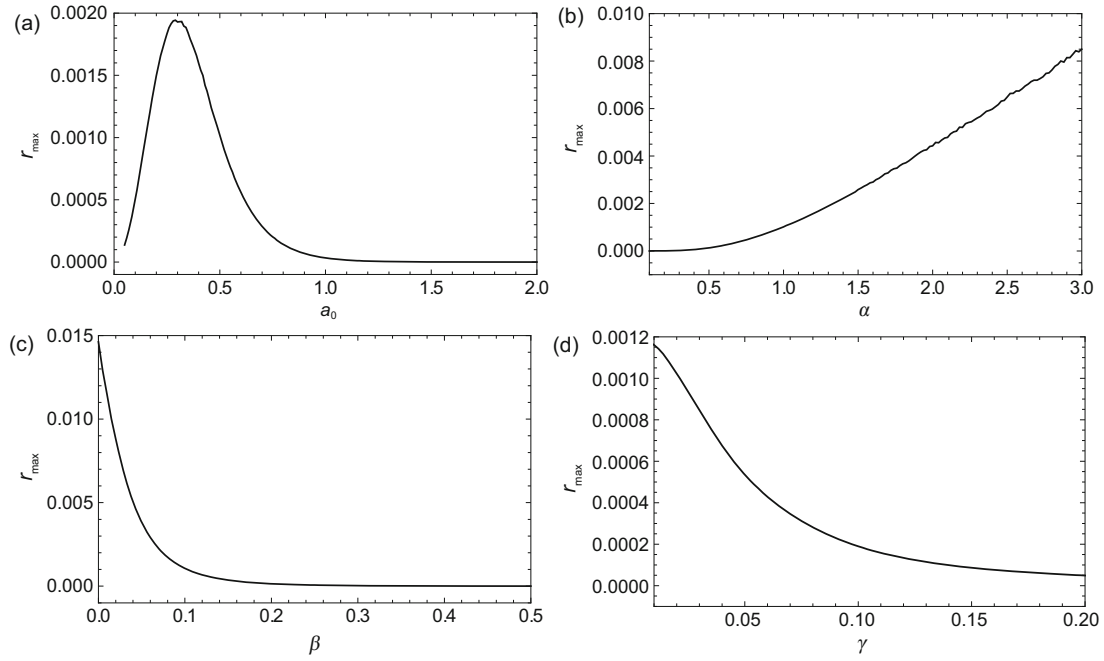

Fig. 11 Effect of parameters a_0 (a), α (b), β (c), and γ (d) on the maximal cross-correlation between X_{10} and X_0

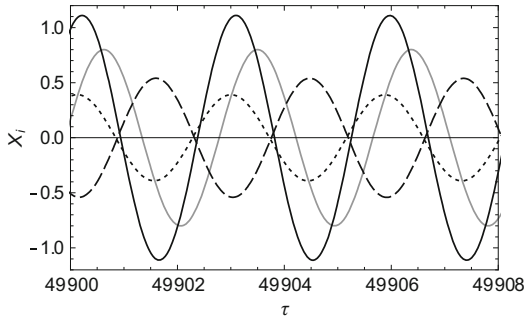

Fig. 12 Vibrations of the system ($n = 10$) for $\Omega_{ex} \approx 2.184$ and $a_0 = 0.8$: X_0 (solid, grey), $X_8 \times 10^3$ (solid, black), $X_9 \times 10^3$ (dashed), and $X_{10} \times 10^3$ (dotted)

experiments do not exhibit any variation of the vibration adjustment with a_0, α, β, and γ in the in-phase regime (low Ω_{ex}). Moreover, several selected changes in the initial uniform displacement (X_{i0}) do not cause any noticeable improvement of the phase or amplitude adjustment in both the in-phase and anti-phase cases.

As mentioned before, the studies require long-term analysis of the system dynamics. In the case of $n = 3$, it is sufficient to solve the problem for $0 \le \tau \le 3 \times 10^3$. For $n = 10$, in turn, the steady-state behavior is achievable within the range $0 \le \tau \le 2 \times 10^4$. Obviously, cross-correlation is an approximate tool for assessment of the phase adjustment rate. Some fluctuations and non-smooth changes that arise in the graphs may be of a numerical nature.

To gain a deeper insight into the effect of particular parameters on the synchronization rate, values of $\Delta\tau_{max}$ are evaluated in various parameter planes for $n = 3$. The resulting filled contour plots, related to the cross-correlation between X_3 and X_0, are presented in Fig. 13. For example, Fig. 13a shows a grey scale map on the plane (α, Ω_{ex}). Each cell is a rectangle of dimensions $\Delta\alpha \times \Delta\Omega_{ex}$. Note that the parameter steps may be larger than before (e.g., $\Delta\alpha = 0.05$). Resolution of the maps is adjusted based on the time range necessary for analysis of the system evolution and computation time. The regions filled with white, light grey, and dark grey correspond to the in-phase vibrations of the both oscillators, while the middle grey areas indicate the anti-phase motion.

When it comes to the plane (α, Ω_{ex}), there are two subregions of the in-phase state (Fig. 13a). The first one, at low values of the excitation frequency, relates to the prediction Eq. (35). Above the second region (tongue), one can observe a transition curve that corresponds to parabola described by Eq. (35). On the parameter plane (β, Ω_{ex}), such evident bands of the in-phase motion can also be observed (Fig. 13b).

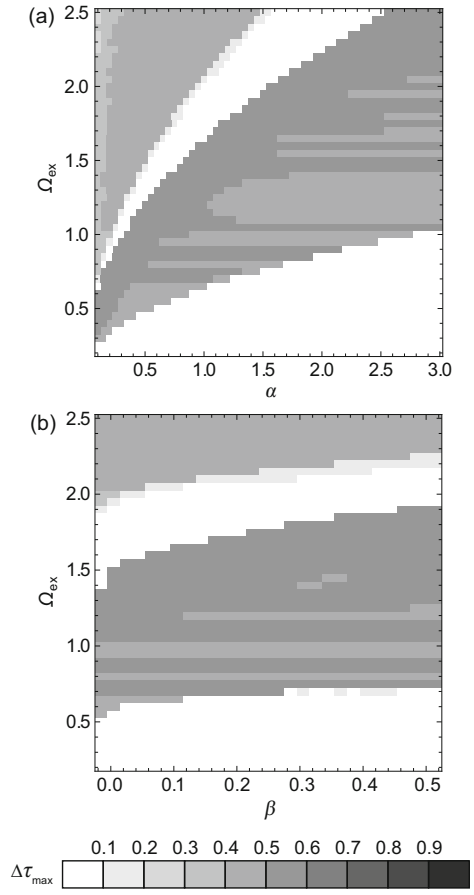

Fig. 13 Effect of parameters α, β, and Ω_{ex} on the cross-correlation between X_3 and X_0: time shift $\Delta\tau_{max}$ on the parameter planes (α, Ω_{ex}) (a) and (β, Ω_{ex}) (b) ($n = 3$)

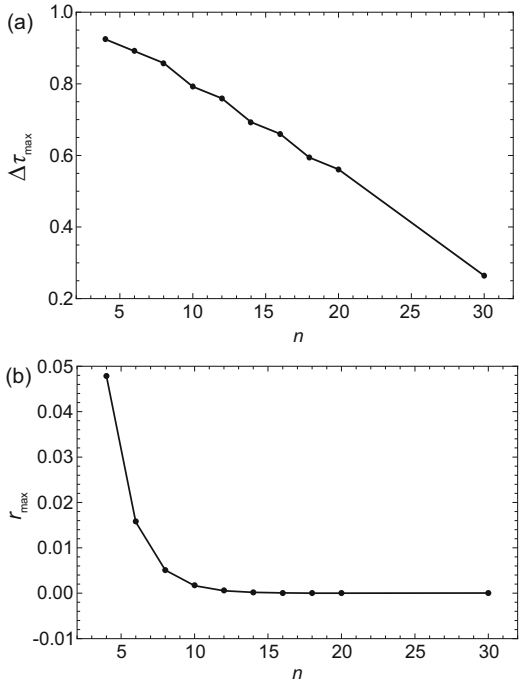

Fig. 14 Effect of the number of oscillators n on the cross-correlation between X_n and X_0: (a) time shift $\Delta\tau_{max}$; (b) the maximal cross-correlation r_{max} ($\Omega_{ex} = 2.074$)

Because $a_0 < 1$, the dependence between β and the critical values of Ω_{ex} is much weaker.

Finally, the effect of the number of oscillators on the synchronization rate is analyzed for the anti-phase steady-state. Results based on the analysis of cross-correlation between X_n and X_0 are shown in Fig. 14. As can be seen, time shift $\Delta\tau_{max}$ decreases quasi-linearly with growing n. Note that the results are obtained for even n, and thus, an acceptable phase adjustment is reached when $\Delta\tau_{max} > 0.75$ or $\Delta\tau_{max} < 0.25$. For the given system, such a situation occurs for $n < 14$ and $n > 30$. The latter case does not seem very attractive, because the vibration amplitude of the last element declines exponentially with increasing n.

All the numerical experiments are performed by means of the MEBDFV solver based on the modified extended backward differentiation formulas (MEBDF) developed by Cash (1983; 2003). This advanced code is an efficient tool, especially for the dynamic simulation of nonlinear multi-body systems described by large sets of implicit differential equations (IDEs) (Mazzia and Magherini, 2003; Fritzkowski and Kamiński, 2009).

4.2 Mechanical system with friction

Let us now report some observations on the chain system with dry friction. Assume that the contact between the oscillators and the ground is characterized by a constant friction coefficient μ. Using the classical Coulomb model, equations of motion Eq. (6) should be enriched with the friction forces:

$$F_i^{\mathrm{FR}} = -\mu m_i g \operatorname{sgn}(\dot{x}_i), \tag{41}$$

where $i = 1, 2, \cdots, n$. After non-dimensionalization, they take the form of

$$f_i^{\mathrm{FR}} = -\mu \operatorname{sgn}(\dot{X}_i). \tag{42}$$

With an application of the averaging method, dynamical systems involving this type of nonlinearity are analyzed (McLachlan, 1950; Hoffmann *et al.*, 2004). However, in the context of long-time numerical integration, to eliminate burdensome difficulties

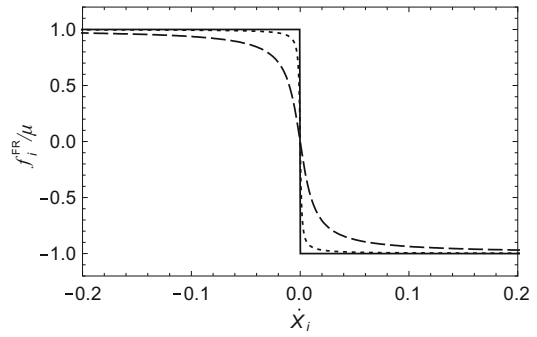

Fig. 15 Approximations of the friction force: the pure Coulomb model (solid), $\eta = 10^2$ (dashed), and $\eta = 10^3$ (dotted)

associated with the discontinuities, a simple smoothing technique is used. The friction forces Eq. (42) are replaced with

$$f_i^{\mathrm{FR}} = -\frac{2\mu}{\pi}\arctan(\eta\dot{X}_i), \tag{43}$$

where η is an accuracy parameter. Such an approach is applied to more sophisticated and alternate friction models (Galvanetto *et al.*, 1995; Leine *et al.*, 1998; van de Vrande *et al.*, 1999).

The smooth functions Eq. (43) with $\eta = 10^2$ and $\eta = 10^3$ are depicted in Fig. 15. Increasing the value of η improves the approximation but simultaneously intensifies the steep slope at $\dot{X}_i = 0$. Nevertheless, the MEBDFV solver is capable of dealing with this issue. In our numerical simulations, $\eta = 10^5$.

When considering the system with friction, the effect naturally seems to be rather an obstacle for synchronous motion. Apart from the visco-elastic couplings and the excitation, friction becomes one more factor leading towards complicated dynamics. It is obvious that the discussed regularity of motion can be easily disturbed, since stick-slip vibrations can introduce disorder into the interactions between neighbors. The relation of the excitation strength (amplitude) to the friction coefficient becomes crucial.

As an example, consider a system of $n = 10$ elements with $\mu = 0.05$. Fig. 16 shows the displacement range ($i = 6$, 8, 10)

$$\Delta X_i = X_i^{\max} - X_i^{\min}, \tag{44}$$

versus amplitude a_0. The results are obtained for Eq. (33), $\Omega_{\mathrm{ex}} = 0.1$, and zero initial positions ($X_{i0} = 0$). The maximal and minimal displacements are found within a few periods T at the steady-state

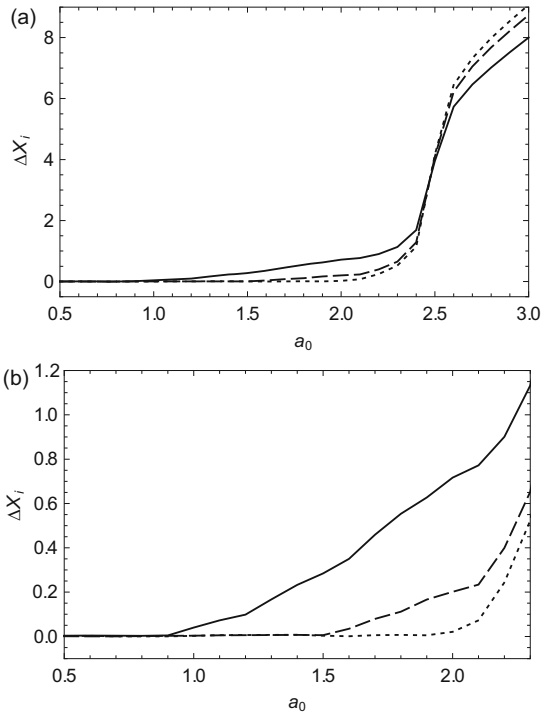

Fig. 16 Full view (a) and clipped view (b) of the effect of a_0 on the range of displacements: ΔX_6 (solid), ΔX_8 (dashed), and ΔX_{10} (dotted) ($\Omega_{\mathrm{ex}} = 0.1$)

phase of motion. The graph indicates that the oscillators are consecutively 'activated' because of an increase in a_0. The nth member starts moving lastly. Even for such a low value of μ, it is required that $a_0 > 2$ to excite the whole chain, i.e., to ensure vibration of all members with practically meaningful amplitudes.

The adjustment between particular oscillators and the excitation for $a_0 = 2.5$ and $a_0 = 5$ can be assessed on the basis of Fig. 17. Understandably, in both cases evident phase shifts occur which are not presented in the system without friction (Fig. 7a). However, the adjustment grows with the excitation amplitude.

The importance of a proper selection of a_0 and μ can be also revealed by an analysis of the cross-correlations $r_{i,0}$. Consider, for instance, $\Delta\tau_{\max}$ and $r_{\max}$ as functions of the friction coefficient. These two characteristics corresponding to the last member ($i = 10$), computed for $a_0 = 2.5$ and $\Omega_{\mathrm{ex}} = 0.1$ are presented in Fig. 18. Over a narrow range ($0 < \mu \leq 0.06$), the phase adjustment between X_{10} and X_0 constantly declines with μ. For $\mu > 0.06$ the time shift undergoes more rapid changes, but simultaneously $r_{\max}$ drops close to 0. Thus, the vibration

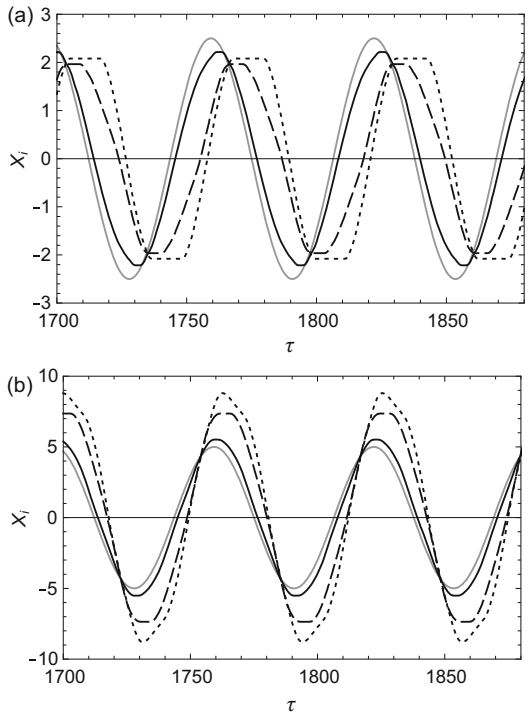

Fig. 17 Vibrations of the system ($n = 10$) for $\Omega_{ex} = 0.1$ and $a_0 = 2.5$ (a), $a_0 = 5$ (b): X_0 (solid, grey), X_1 (solid, black), X_5 (dashed), and X_{10} (dotted)

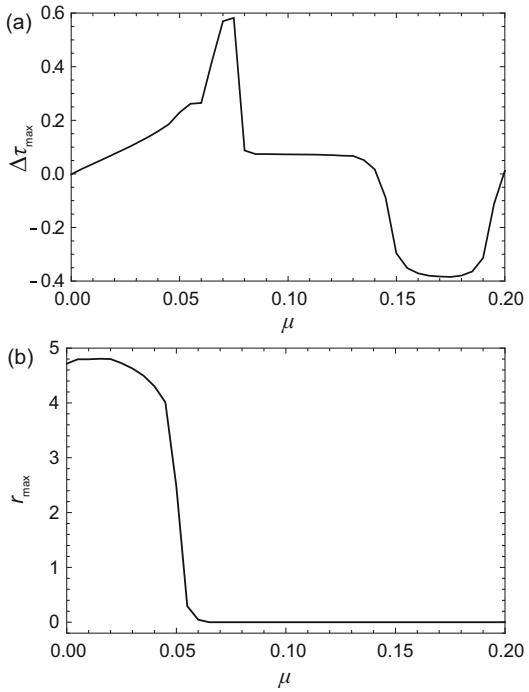

Fig. 18 Effect of friction coefficient μ on the phase adjustment of X_{10} and X_0: (a) time shift; (b) the maximal cross-correlation ($a_0 = 2.5$, $\Omega_{ex} = 0.1$)

becomes negligible.

As can be concluded from the discussed examples, the interplays between particular parameters are really complex, and their detailed analysis requires extensive computational effort. Apart from the effects discussed in the case of the system without friction, some new factors arise: the threshold excitation amplitude for generation of steady-state vibration along the entire chain, the interaction between viscous damping and dry friction, etc. It is worth mentioning that, according to preliminary results, the anti-phase state seems much harder to achieve. Even for weak friction, very fast varying excitation is rather incapable of forcing constant vibrational motion (especially of the last member). All these issues are not thoroughly addressed in this paper.

5 Conclusions

In this paper, a 1D chain of coupled oscillators has been considered, including the Duffing-type nonlinearity, viscous damping, and kinematic harmonic excitation. The equations of motion have been presented in a non-dimensional form. The approximate equations for the vibrational amplitudes and phases have been derived using the averaging method. A simple analysis has enabled the determination of two synchronous regimes: the in-phase state (for low excitation frequency) and the anti-phase state (for high excitation frequency). The validity of these predictions has been examined by a series of numerical studies. The effect of the model parameters on the rate of synchronization has been analyzed.

To sum up, the prediction related to the in-phase regime is quite trivial, and works well for multi-degree-of-freedom chains. Since the first natural frequency of the abbreviated (linear) system decreases with the number of members n, the excitation frequency Ω_{ex} has to be considerably lowered for a large n. Understandably, the amplitude adjustment grows as $\Omega_{ex} \to 0$.

The other, less banal prediction of the anti-phase motion is valid in the case of short chains ($n < 14$). The phase shift between the consecutive oscillators response and the excitation increases linearly with growing n. The prediction for any number of oscillators is correct in the sense that the phase adjustment of the neighboring oscillators remains very high. The synchronization rate between the system members and the excitation can be slightly improved by increasing the strength of the excitation and/or

the nonlinear coupling. However, the oscillation amplitudes significantly drop with growing a_0 and β. Consequently, the recipe for the improvement may lose its practical meaning due to vibration decay of the last elements.

In the case of the system with friction, the considerations become much more complicated. One of the most important issues is to determine the minimal amplitude a_0 which is sufficient to generate vibrations of all members.

Limitations of the predictions may be caused by various factors. First of all, the averaging method is one of the simplest approximate analytical tools. Usually it is applied to relatively simple weakly nonlinear systems with just a few degrees of freedom. Secondly, there are two important issues that have not been elaborated, but may be crucial: stability of solutions and sensitivity of the system to initial conditions. Determination of stability and instability regions as well as basins of attraction on parameter planes can cast a new light on the range of applicability of the analytical predictions.

Obviously, there are also other problems that have not been addressed in this work, e.g., the interplay between two types of dissipation (viscous damping and dry friction), or the relation between the synchronous states and wave phenomena in the corresponding continuous system. However, the presented results can serve as a good basis for more detailed investigations.

References

Balanov, A., Janson, N., Postnov, D., *et al.*, 2009. Synchronization: from Simple to Complex. Springer, Berlin, Germany.

Belykh, V.N., Osipov, G.V., Kuckländer, N., *et al.*, 2005. Automatic control of phase synchronization in coupled complex oscillators. *Physica D: Nonlinear Phenomena*, **200**(1-2):81-104. http://dx.doi.org/10.1016/j.physd.2004.10.008

Cash, J.R., 1983. The integration of stiff initial value problems in odes using modified extended backward differentiation formulate. *Computers & Mathematics with Applications*, **9**(5):645-657. http://dx.doi.org/10.1016/0898-1221(83)90122-0

Cash, J.R., 2003. Efficient numerical methods for the solution of stiff initial-value problems and differential algebraic equations. *Proceedings of the Royal Society of London A: Mathematical, Physical and Engineering Sciences*, **459**:797-815. http://dx.doi.org/10.1098/rspa.2003.1130

Fritzkowski, P., Kamiński, H., 2009. Dynamics of a rope modeled as a discrete system with extensible members. *Computational Mechanics*, **44**(4):473-480. http://dx.doi.org/10.1007/s00466-009-0387-2

Galvanetto, U., Bishop, S.R., Briseghella, L., 1995. Mechanical stick-slip vibrations. *International Journal of Bifurcation and Chaos*, **5**(3):637-651. http://dx.doi.org/10.1142/S0218127495000508

Hoffmann, N., Bieser, S., Gaul, L., 2004. Harmonic balance and averaging techniques for stick-slip limit-cycle determination in mode-coupling friction self-excited systems. *Technische Mechanik*, **24**(3-4):185-197.

Kryloff, N., Bogoliuboff, N., 1947. Introduction to Nonlinear Mechanics. Princeton University Press, Princeton, USA.

Leine, R.I., van Campen, D.H., de Kraker, A., *et al.*, 1998. Stick-slip vibrations induced by alternate friction models. *Nonlinear Dynamics*, **16**(1):41-54. http://dx.doi.org/10.1023/A:1008289604683

Mazzia, F., Magherini, C., 2003. Test Set for Initial Value Problem Solvers. Department of Mathematics, University of Bari, Italy.

McLachlan, N.W., 1950. Ordinary Non-linear Differential Equations in Engineering and Physical Sciences. Oxford University Press, London, UK. http://dx.doi.org/10.1049/sqj.1951.0035

Minorsky, N., 1947. Introduction to Non-linear Mechanics. Edwards Brothers, Ann Arbor, USA.

Nayfeh, A.H., Mook, D.T., 1995. Nonlinear Oscillations. Wiley, New York, USA.

Osipov, G.V., Kurths, J., Zhou, C., 2007. Synchronization in Oscillatory Networks. Springer, Berlin, Germany. http://dx.doi.org/10.1007/978-3-540-71269-5

Sanders, J.A., Verhulst, F., 1985. Averaging Methods in Nonlinear Dynamical Systems. Springer, New York, USA. http://dx.doi.org/10.1007/978-0-387-48918-6

van de Vrande, B.L., van Campen, D.H., de Kraker, A., 1999. An approximate analysis of dry-friction-induced stick-slip vibratons by a smoothing procedure. *Nonlinear Dynamics*, **19**(2):157-169. http://dx.doi.org/10.1023/A:1008306327781

中文概要

题　目：耦合非线性振子链的周期性驱动动力学研究

目　的：考虑一个包含Duffing型非线性、粘性阻尼和运动谐波激励的一维耦合振子链，本文旨在推导描述振幅和相位的近似方程，得到并检验两类基本共振态（同相共振和反相共振）发生的条件，同时分析模型参数对同步率的影响。

创新点：1. 利用时间序列的互相关测量特定振子间的相位蝶，并通过一系列的数值实验来验证理论预测的结果；2. 给出考虑干摩擦的系统共振的一些简要说明。

方　法：1. 采用经典的平均值法进行理论分析；2. 采用MEBDFV求解器计算多自由度系统的数值解。

结　论：1. 利用平均值法确定了两种共振现象：同相状态（低频激励）和反相状态（高频激励）；2. 关于同相共振的预测非常琐碎但对多自由度的振子链非常适用；3. 对于反相共振的预测适用于短的振子链；4. 可以通过改变系统的物理参数来提高同步率。

关键词：耦合非线性振子；同步运动；平均值法